Measurement Based Identification of MPCs in an Urban Drone-to-Drone Propagation Scenario

Dennis Becker*, Uwe-Carsten Fiebig*,
*Institute of Communications and Navigation
German Aerospace Center (DLR)
Oberpfaffenhofen-Wessling, Germany
dennis.becker@dlr.de

***Abstract*—The risk of mid-air collisions between flying drones has to be minimized to the greatest possible extent as it endangers people in the air and on the ground especially when being integrated into dense urban airspace. For a safe and efficient operation drones will need to exchange information in a robust and reliable manner and one essential part will be direct Drone-to-Drone (D2D) communications. Especially, for dense drone scenarios in urban environments a communication system must cope with the specific underlying channel propagation conditions. In previous works, in order to characterize the propagation effects between two moving drones in urban environments, we performed a channel sounding measurement campaign and presented an approach to localize the origin of the measured multipath components (MPCs) for a three-dimensional layout. In this work, we apply this approach on our measured flight scenarios in three different environments in order to identify the MPCs by assigning them to real-world objects. Furthermore, we describe first characteristics for them and show that the measured urban scenario consists of different kinds of components that must be considered in a future D2D channel model.**

***Index Terms*—unmanned aerial vehicle, air-to-air, propagation, drone-to-drone communication, scatterer localization, mpc identification**

I. Introduction

The current, worldwide developments and plans for Urban Air Mobility (UAM) will lead to a highly frequented, urban airspace with automated or autonomously flying drones. The traffic management of the urban air space with unmanned airborne vehicles will have to be carried out differently than it is currently handled in civil aviation due to expected high traffic densities and short reaction times needed in dense urban environments, which make the remote control of unmanned aerial vehicles (UAVs) unfeasible. The traffic management will rather rely on pre-planned, conflict-free trajectories and their continuous monitoring. The realization of such a concept may be based on existing communication technologies and infrastructure such as cellular communications. Under ideal conditions, this approach seems sufficient at first, but on closer inspection, weaknesses become visible, such as a lack of redundancy or a missing higher-level safety net as it is common in todays civil aviation and ship traffic and already planned for the future autonomous driving. Therefore, we see the need to introduce an additional, decentralized and robust communications concept that enables a reliable information exchange of position data and trajectories directly between UAVs in order to avoid collisions between all urban airspace users. To the best of our knowledge, there is currently no commercial communication system available that addresses the future requirements for the safe and efficient information exchange between flying vehicles while considering the specific and challenging signal propagation characteristics in urban environments. Therefore, we conducted a wideband channel measurement campaign in order to measure the D2D propagation conditions in an urban scenario with small sized hexacopters and presented a novel measurement setup that overcomes limitations resulting from size, weight and power constraints [1], [2]. Furthermore, we discussed two different approaches in order to identify the MPC sources and showed that it is feasible to localize them by a joint delay and Doppler frequency parameter estimation that is transformed into the 3D domain and intersected with 3D geometry data of the environment [3].

In this paper we apply the localization approach on measurements for three different environments with several different flight paths and identify the MPC sources by assigning them to the real-world objects that most probably caused them and evaluate the characteristics of them. The results will be used for a specific geometrical based stochastic channel model (GSCM) for D2D propagation in urban scenarios and will help to increase robustness in the development of a D2D communications system.

II. Measurement Campaign

We performed the world-wide first wideband channel sounding measurement campaign with two small hexacopters at C-Band in an urban scenario for D2D propagation at our site in Oberpfaffenhofen, Germany. In order to measure as much as possible different propagation effects we choose three different environments with different flight trajectories and planned critical scenarios in which two communicating drones are not always in line of sight (LOS) to each other and are on a collision course. The scenarios are described in more detail in [2], but the all trajectories in the three environments can be seen in Fig. 1, Fig. 2 and Fig. 3.

A. Measurement Environment

Environment A provides relative tall buildings around 20 m height standing close together with an urban canyon. Fig. 1

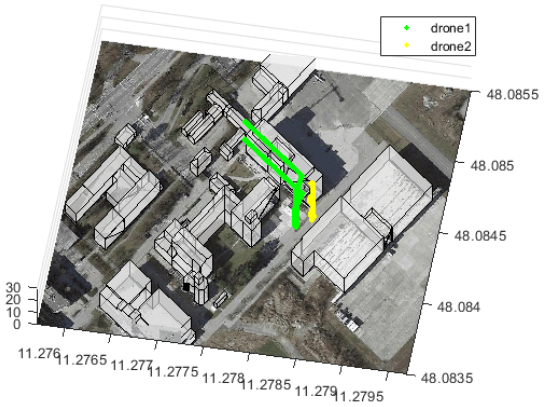

Fig. 1. **Environment A** with different flight trajectories for both drones in several scenarios.

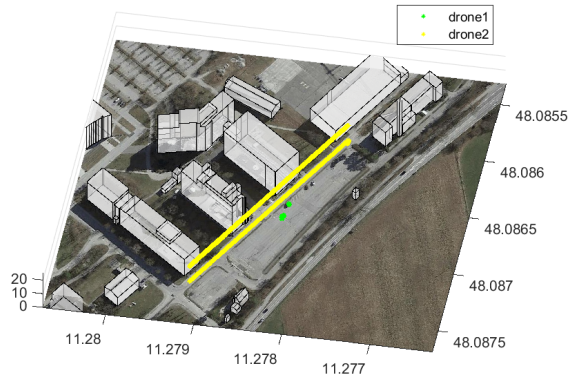

Fig. 3. **Environment C** with different flight trajectories for both drones in several scenarios.

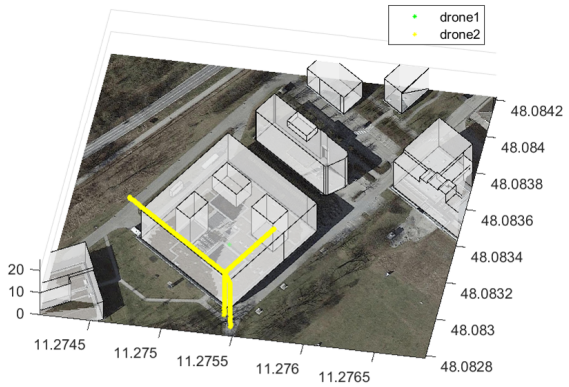

Fig. 2. **Environment B** with different flight trajectories for both drones in several scenarios.

shows the flown trajectories and the 3D geometry of the buildings plotted on top of a 2D satellite image. Here we have measured 6 different scenarios in which the drones fly below and above rooftop altitudes. For some scenarios, the drones are not in visual line-of-sight of each other. At the environment B shown in fig. 2 we have measured two scenarios. The first scenario is a horizontal flight of one drone close to the building at two different heights while the second drone hovers inside a courtyard at different heights. On the second scenario the first hovering drone is also moving vertically up and down the courtyard simulating a start or landing scenario. Note that the actual courtyard is missing in the 3D geometry database beside the other three, but the transparent overlap on the satellite image reveals the location of it. Environment C provides a relative long street along different buildings and is illustrated in Fig. 3. These different environments with varying surrounding obstacles make it possible to measure different kinds of MPCs.

B. Measurement Setup

The whole measurement equipment and setup was presented in more details in [1]. Tab. I summarizes the most important parameters of our measurement system. We performed measurements in the C-Band at 5.2 GHz with 100 MHz bandwidth. With the given setup we are able to resolve MPCs with propagation delays of up to 12.8 μs in steps of 10 ns, resulting in a spatial resolution of down to 3m and a resolvable distance up to 1920 m for which the dynamic range of 52 dB is also sufficient. Given a snapshot rate of 1.024 ms, the maximum resolvable Doppler frequency is 488 Hz, which is sufficient as the drones moved with speeds up to 1m/s. The omni-directional and vertical polarized radiating antennas were mounted below the drones.

TABLE I
CHANNEL SOUNDING PARAMETER

Parameter	Symbol	Value
Center frequency	f_c	5.2 GHz
Bandwidth	B	100 MHz
Tx Power	P_{tx}	30 dBm
Signal duration	T_p	12.8 μs
Signal period	T_g	1.024 ms
Max resolvable Doppler freq.	$f_{d_{\text{max}}}$	488 Hz
ADC resolution	res_{adc}	8 bit
Dynamic range	α_{agc}	52 dB
Antenna Tx		omni-dir. V-polarized 0 dBi
Antenna Rx		omni-dir. V-polarized 0 dBi

III. METHOD

For the identification of the measured MPCs we make use of the scatterer localization approach for 3 dimensional layouts as presented in [3] that was also applied for 2D cases in [4]–[6]. Within the approach we jointly estimate the delay and Doppler frequency probability density function (PDF) and transform into a 3D Cartesian domain and intersect the results with known objects given by 2D satellite images, from 3D geometry data obtained from land surveying offices or a combination of both. Due to the 3D layout of the environment for the drone scenarios a simpler 2D projection will not work and most probably lead to false locations, when the scatterer are not in a plane with the drones. The parameters can be estimated and tracked with algorithms like Kalman enhanced super resolution tracking algorithm (KEST) that was introduced in [7]. The results often lead to ambiguous locations for every measurement snapshot, but if the true location does not move

too much or if it is a perfect point scatterer, then it is possible to average out the ambiguities. Therefore, we first analyze the moving behavior for each MPC for several snapshots and then enhance the localization only for the point scatterers. Nevertheless in most cases there is only one intersection with a real world object and the ambiguous location estimate can be identified. Furthermore, it is not necessary to analyze the whole measurement data set with a huge computational effort, because the flight patterns repeat and it is possible for most scenarios to visually inspect the channel impulse responses and recognize the same MPCs at different snapshots. Therefore we analyzed segments of the measurements containing all detectable MPCs. We demonstrate this method on one flight scenario at environment C. Fig. 4 shows the channel impulse response for the whole measured flight and three segments that are analyzed. The white horizontal lines help to visualize four segments in which the two drones fly on similar paths. For the estimated delay and Doppler frequency parameter for each detected MPC, we estimate the locations for several snapshots and assign them to real world objects. Fig. 5 illustrates the locations of the detected MPCs these locations together with the according flight trajectories. They are identified according to the results in Tab. IV. Thereby, the location estimates for all point scatterers are enhanced by averaging over the indicated snapshot intervals. Red colors indicate locations with high probability For the line-of-sight component, no location estimate intersects with the surroundings as it accounts for the direct signal path. We apply this method to several flight scenarios at the three different environments and combine the location estimates.

IV. Results and Discussion

When combining the results for different flight scenarios at each environment, some detected MPCs in the measurements might result from the same sources. In this case, the location estimate can be further enhanced if the MPC was measured from different positions and flight directions. Fig. 6 illustrates all MPCs that are identified in Tab. II for environment A. Here quite a lot of scatterers are located at the rooftop of building B160, which are metallic objects like steelbeams, parts of air conditioner systems and metallic tubes. But we can also identify a good reflecting rooftop on building B140. Only MPC10 is not clearly identifiable as it might most presumably caused by a reflecting surface of the distant building, but the source can also be an object on the rooftop of another building and the source location is moving. Note that in this scenario many MPCs with close distance to the drones in the urban canyon might not be resolvable and overlap with the line-of-sight component. For this the fading statistics must be analyzed in more details. At environment B, the localization of the scatterer is hardly possible as the drones are not in LOS and the drone in the courtyard receives signals reflected from the surrounding walls. The source location for MPC1 changes, but stays close to the rooftop edge of the courtyard. At some snapshots in the measurements some weak, probably diffracted parts of the LOS component can be identified, but

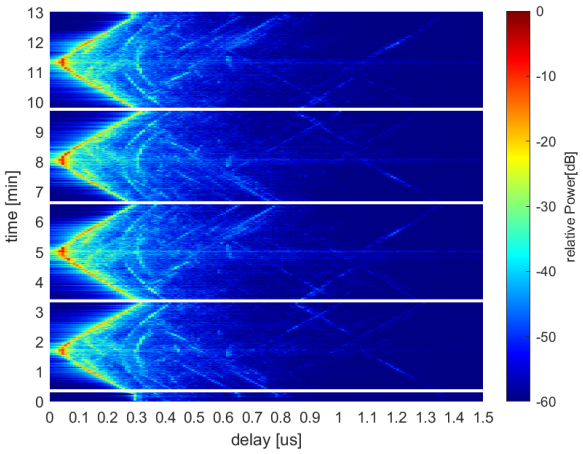

(a) **Full measured flight**

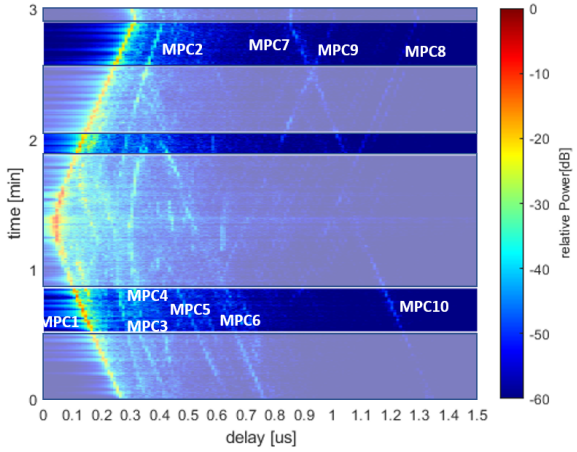

(b) **Excerpt with three segments**

Fig. 4. Channel Impulse Response with indicated MPCs for one flight at environment C. The visible MPCs in the excerpt can be clearly seen again at other segments. The parameters are analyzed within three regions.

TABLE II
Identified Multipath Components at Environment A

Name	Source Object	Type
MPC1	LOS	line-of-sight component
MPC2	Bikestation roof	point scatterer
MPC3	Roof edge	point scatterer
MPC4	Roof object1	point scatterer
MPC5	Roof object2	point scatterer
MPC6	Steelbeam1	point scatterer
MPC7	Steelbeam2	point scatterer
MPC8	Steelbeam3	point scatterer
MPC9	Rooftop	surface reflection
MPC10	Building surface	surface reflection

are not visible as locations here. When adding measurements in environment C to the already described scenario, new scatterers are identified and the location estimates of already identified ones are enhanced. At this environment quite a lot of street lamps on the long street could be identified, but also parts of a surrounding fence of the campus site were identified as point scatterers. Overall, we can identify most

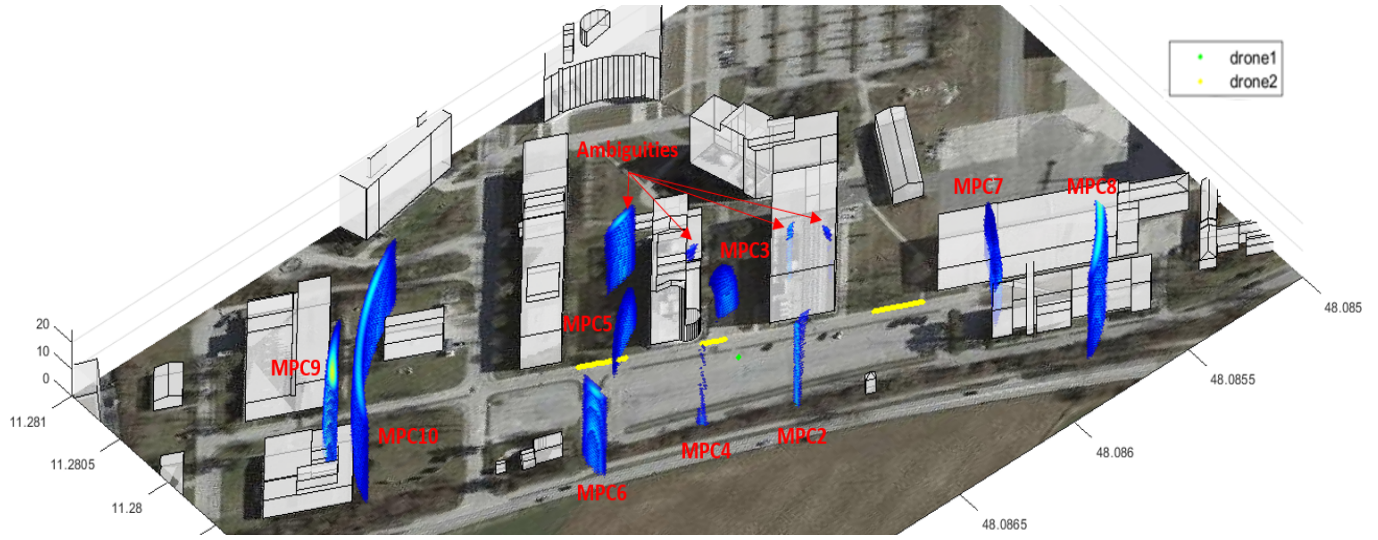

Fig. 5. Environment C with estimates of the scatterer's locations for 10 different MPCs that are shown in the measurements.

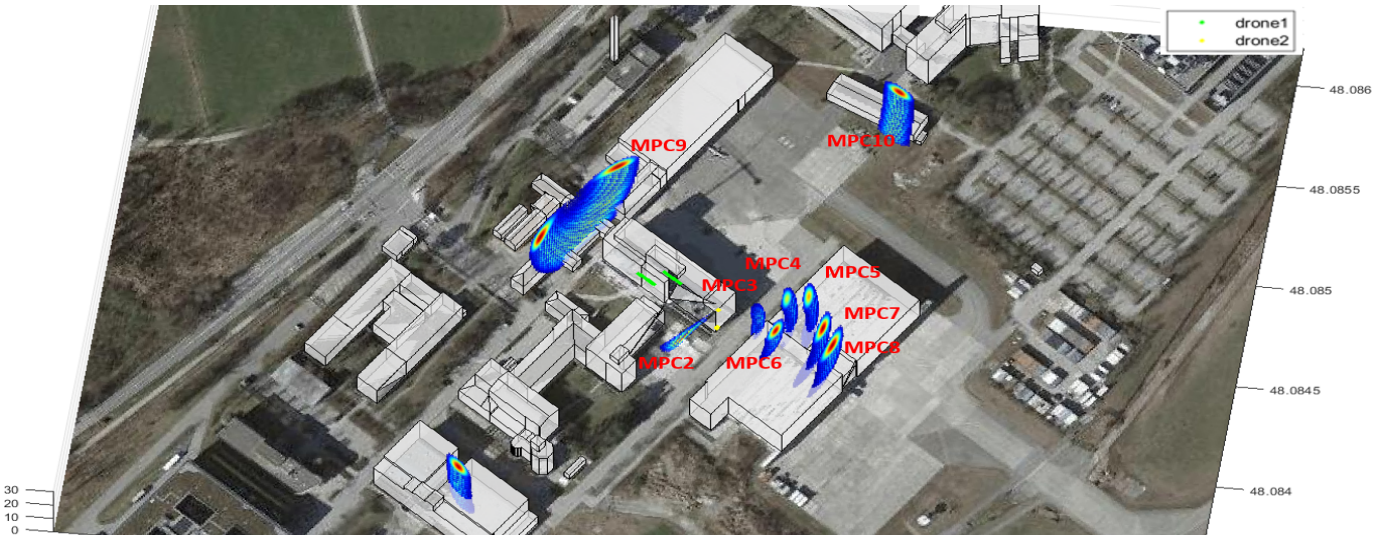

Fig. 6. Location estimates for all analyzed MPCs and drone flight trajectories at Environment A.

TABLE III
IDENTIFIED MULTIPATH COMPONENTS AT ENVIRONMENT B

Name	Source Object	Type
MPC1	Roof edge	reflection
MPC2	Roof object	point scatterer

of the detected and analyzed MPCs from the measurements with meaningfull source locations. Sometimes we can see moving surface reflections at the ground and buildings, but the majority of the components are point scatterers that are only moving within measurement uncertainties and the source objects for scattering are mostly metallic objects like fences, railings, street lamps, metallic rooftop elements. This outcome is expected as these objects have good reflection properties for electromagnetic waves.

V. CONCLUSION

Results show that the scatterer locations could be identified in a three-dimensional layout from the measurement data although for some MPCs it is not easy to identify the origin due to ambiguities in the location estimates. Mostly point scatterer from metallic objects were identified, but also long term reflectors at some building surfaces and on the ground are present. This identification is possible by only analyzing excerpts from the measurements. By having assigned real-world objects to the detected MPCs and with known scatterer locations we can now derive further statistics for them. Therefore, this is an essential step towards the definition of a channel model for D2D propagation in urban environments.

REFERENCES

[1] D. Becker and L. Schalk, "Enabling Air-to-Air Wideband Channel Measurements between Small Unmanned Aerial Vehicles with Optical

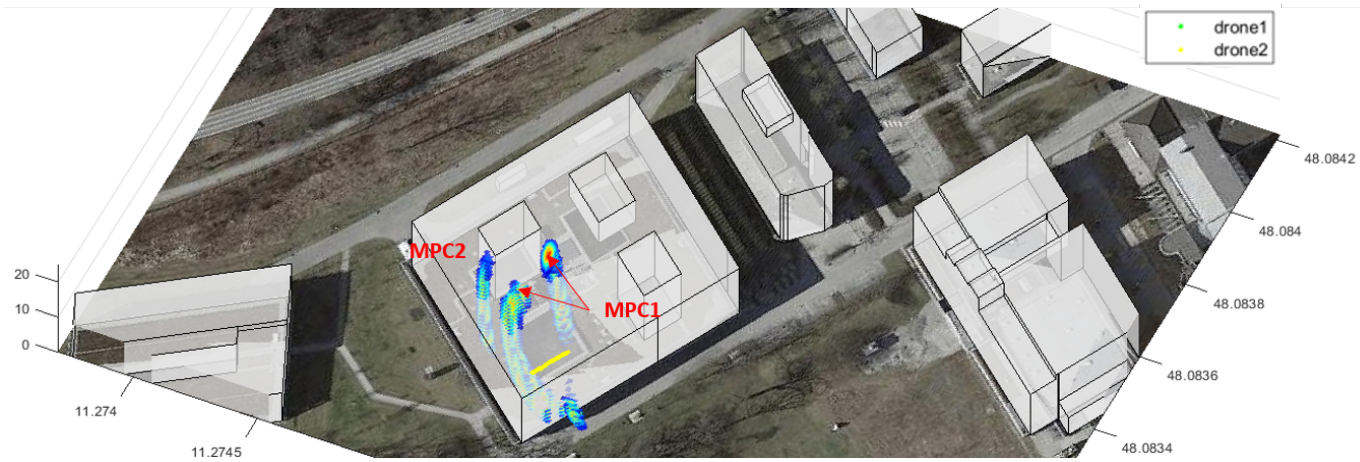

Fig. 7. Location estimates for all analyzed MPCs and drone flight trajectories at Environment B.

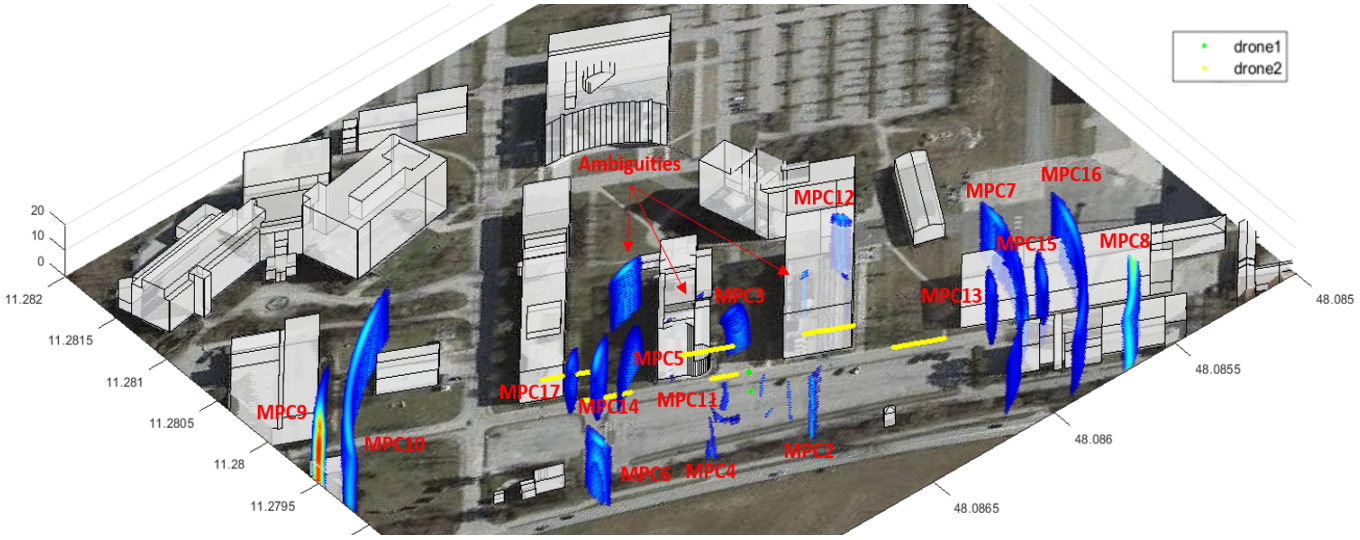

Fig. 8. Location estimates for all analyzed MPCs and drone flight trajectories at Environment C.

Fibers," 2019 IEEE/AIAA 38th Digital Avionics Systems Conference (DASC), San Diego, CA, USA, 2019, pp. 1-7

[2] D. Becker, U. Fiebig and L. Schalk, "Wideband Channel Measurements and First Findings for Low Altitude Drone-to-Drone Links in an Urban Scenario," 2020 14th European Conference on Antennas and Propagation (EuCAP), Copenhagen, Denmark, 2020, pp. 1-5

[3] D. Becker, U.-C. Fiebig, and L. M. Schalk, "Approach for Localizing Scatterers in Urban Drone-to-Drone Propagation Environments," in 2021 15th European Conference on Antennas and Propagation (EuCAP), Dusseldorf, Germany, Mar. 2021, pp. 1–5.

[4] N. Schneckenburger et al., "Reflector localization for geometrical modeling the air-ground channel," IEEE Transactions on Vehicular Technology, pp. 1–1, 2018

[5] Unterhuber, Paul and Walter, Michael and Schneckenburger, Nicolas and Kürner, Thomas, "Joint Delay and Doppler Frequency Estimation for Scatterer Localization in Railway Environments", 13th European Conference on Antennas and Propagation, EuCAP 2019

[6] I. Rashdan, F. Ponte Müller, S. Sand, T. Jost, and G. Caire, "Measurement-based geometrical characterisation of the vehicle-to-vulnerable-road-user communication channel," IET Microwaves, Antennas amp; Propagation, vol. 14, no. 14, pp. 1700–1710, Nov. 2020.

[7] T. Jost, W. Wang, U. C. Fiebig, and F. Perez-Fontan, "Detection and Tracking of Mobile Propagation Channel Paths," IEEE Transactions on Antennas and Propagation, vol. 60, no. 10, pp. 4875–4883, Oct 2012.

TABLE IV
IDENTIFIED MULTIPATH COMPONENTS AT ENVIRONMENT C

Name	Source Object	Type
MPC1	LOS	line-of-sight component
MPC2	Fence1	point scatterer
MPC3	Railing	point scatterer
MPC4	Fence2	point scatterer
MPC5	Streetlamp1	point scatterer
MPC6	Fence3	point scatterer
MPC7	Rooftop1	point scatterer
MPC8	Sign1	point scatterer
MPC9	Rooftop2	point scatterer
MPC10	Building	surface reflection
MPC11	GREF	ground surface reflection
MPC12	Rooftop object	point scatterer
MPC13	Streetlamp2	point scatterer
MPC14	Streetlamp3	point scatterer
MPC15	Sign2	point scatterer
MPC16	Rooftop3	surface reflection
MPC17	Streetlamp4	point scatterer